doi:10.1016/j.jmb.2011.12.034 J. Mol. Biol. (2012) 415, 866–880

Contents lists available at www.sciencedirect.com

Journal of Molecular Biology

journal homepage: http://ees.elsevier.com.jmb

Nucleocapsid Protein Annealing of a Primer–Template Enhances (+)-Strand DNA Synthesis and Fidelity by HIV-1 Reverse Transcriptase

Jiae Kim[1], Anne Roberts[1], Hua Yuan[2], Yong Xiong[2] and Karen S. Anderson[1]*

[1]*Department of Pharmacology, Yale University School of Medicine, SHM B350B, 333 Cedar Street, New Haven, CT 06520-8066, USA*
[2]*Department of Molecular Biophysics and Biochemistry, Yale University, New Haven, CT 06520-8114, USA*

Received 14 November 2011; received in revised form 9 December 2011; accepted 16 December 2011
Available online 23 December 2011

Edited by J. Karn

Keywords:
HIV-1 reverse transcriptase; HIV-1 nucleocapsid protein; nucleocapsid-facilitated annealing; (+)-strand synthesis; transient kinetics

Human immunodeficiency virus type 1 (HIV-1) requires reverse transcriptase (RT) and HIV-1 nucleocapsid protein (NCp7) for proper viral replication. HIV-1 NCp7 has been shown to enhance various steps in reverse transcription including tRNA initiation and strand transfer, which may be mediated through interactions with RT as well as RNA and DNA oligonucleotides.

With the use of DNA oligonucleotides, we have examined the interaction of NCp7 with RT and the kinetics of reverse transcription during (+)-strand synthesis with an NCp7-facilitated annealed primer–template. Through the use of a pre-steady-state kinetics approach, the NCp7-annealed primer–template has a substantial increase (3- to 7-fold) in the rate of incorporation (k_{pol}) by RT as compared to heat-annealed primer–template with single-nucleotide incorporation. There was also a 2-fold increase in the binding affinity constant (K_d) of the nucleotide. These differences in k_{pol} and K_d were not through direct interactions between HIV-1 RT and NCp7. When extension by RT was examined, the data suggest that the NCp7-annealed primer–template facilitates the formation of a longer product more quickly compared to the heat-annealed primer–template. This enhancement in rate is mediated through interactions with NCp7's zinc fingers and N-terminal domain and nucleic acids. The NCp7-annealed primer–template also enhances the fidelity of RT (3-fold) by slowing the rate of incorporation of an incorrect nucleotide. Taken together, this study elucidates a new role of NCp7 by facilitating DNA-directed DNA synthesis during reverse transcription by HIV-1 RT that may translate into enhanced viral fitness and offers an avenue to exploit for targeted therapeutic intervention against HIV.

*Corresponding author. E-mail address: karen.anderson@yale.edu.
Present address: A. Roberts, Department of Chemistry, Western Connecticut State University, Danbury, CT 06810, USA.

Abbreviations used: HIV-1, human immunodeficiency virus type 1; RT, reverse transcriptase; NCp, nucleocapsid protein; dNTP, deoxynucleoside triphosphate; dCTP, deoxycytidine triphosphate; dTTP, deoxythymidine triphosphate; ESI-TOF MS, electrospray ionization time-of-flight mass spectrometry; MWCO, molecular weight cutoff; EDTA, ethylenediaminetetraacetic acid.

Introduction

The virally encoded enzyme reverse transcriptase (RT) is necessary for the replication of human immunodeficiency virus type 1 (HIV-1). RT is responsible for the conversion of the viral genomic RNA into double-stranded DNA that is subsequently integrated into the host cell's genome. This enzyme is currently one of the major targets for AIDS therapeutics.

Another protein, nucleocapsid protein (NCp), is also necessary for viral replication. Infectious virions contain large amounts of NCps that are believed to have multiple roles in the replication of the RNA genome. These proteins are products from the cleavage of Gag,[1] and two NCps that have been extensively examined are NCp7 and NCp15.[2] NCp7 is considered to be the mature form of the protein. This 55-amino-acid protein contains two zinc finger binding motifs, and the structure has been determined by NMR.[3–5] Deletions of the NCp7 zinc fingers result in noninfectious virus particles that contain less genomic RNA, indicating that the conserved zinc fingers are important for late and early steps of replication.[6] NCp7 binds to both DNA and RNA and has been shown to act as a chaperone to facilitate the annealing of primer and template strands.[7–10] The effects on the presence of NCps during various steps of reverse transcription have been studied.[11–13] These nucleic acid binding proteins have been shown to accelerate (−)-strand DNA transfer during proviral DNA synthesis,[14–16] as well as enhance processivity.[1,9,14,17–20] NCp7 has been shown to help in the fidelity of reverse transcription by preventing mispriming in the PPT region of the genome.[21,22] It has also been established that NCps also play a role in Gag assembly and viral fitness.[1,23]

A number of mechanistic studies have examined the role of NCp7 in RNA-mediated steps including tRNA initiation, strand transfer and (−)-DNA strand synthesis during reverse transcription.[1,9,14–16,20,24–27] It has also been suggested that there is a direct interaction between HIV-1 RT and NCp7.[28,29] However, the effects of NCp7 on the reaction kinetics of reverse transcription during DNA-mediated (+)-strand synthesis using an NCp7-facilitated annealed DNA/DNA primer–template have not been examined in detail. In order to study direct interactions between NCp7 and HIV-1 RT, as well as the binding of RT with an NCp7-facilitated annealed DNA/DNA primer–template resembling PBS(+)/PBS(−), we utilized equilibrium fluorescence spectroscopy. A transient kinetic analysis was then employed to study the effects of using an NCp7-facilitated annealed primer–template upon single-nucleotide incorporation, multiple-nucleotide extension and misincorporation by HIV-1 RT. This methodology allows us to understand what is occurring at the active site of the polymerase and gives us direct information regarding the binding affinity of the incoming nucleotide and the maximum rate of incorporation.[30] These experiments demonstrate that NCp7 enhances single- and multiple-nucleotide incorporation by RT as well as increases the fidelity of this error-prone polymerase. Understanding multiple roles and defining new effects for NCp7 in aiding replication of the viral genome may provide novel avenues to explore in identifying new molecular targets for antiviral therapy.

Results

Purification and analysis of HIV-1 NCp7

HIV-1 NCp7 used for these experiments was purified by a protocol adapted from You and McHenry that utilized a bacterial expression system for production of the recombinant protein and did not indicate a requirement for the addition of exogenous zinc.[31] The protein was analyzed by SDS-PAGE, and a single band was observed at approximately 7 kDa. Protocols using a lyophilized NCp7 protein prepared by chemical synthesis indicated that 3 molar equivalents of zinc sulfate were added.[19] In this study, the purified NCp7 was analyzed by electrospray ionization time-of-flight mass spectrometry (ESI-TOF MS) to determine the zinc metal ligation state of the protein. In the presence of 50 mM ammonium bicarbonate, pH 8, the ESI-TOF spectra indicated that NCp7 has two zinc ions bound to the protein in its native state; therefore, addition of exogenous zinc was not necessary. We observed that the majority of the protein was in the 2 zinc ion state at the +4, +5 and +6 charge states (Supporting Information, Supplemental Fig. S1). At the higher charge states (+5 and +6), a very small amount of the single zinc and no zinc bound forms of the protein were present.

A direct interaction between HIV-1 RT and HIV-1 NCp7

Previous studies using immunoprecipitation/Western blotting and surface plasma resonance have suggested that HIV-1 NCp7 directly interacts with HIV-1 RT[29,32] with submicromolar affinity. In order to quantitatively examine the RT–NCp7 protein–protein interaction, we used fluorescence equilibrium binding.

The equilibrium fluorescence experiments utilized intrinsic protein fluorescence as a signal to observe the protein–protein interaction. HIV-1 RT contains a number of tryptophan residues that may serve as a monitor and allows fluorescence measurements to be determined.[33,34] Changes in the intrinsic protein fluorescence for RT may reflect conformational

changes or binding of a substrate or another protein. In this case, we utilized fluorescence spectroscopy to examine the direct interaction of NCp7 and RT.

Fluorescence was measured at a maximal excitation wavelength of 285 nm and an emission spectrum from 300 nm to 500 nm. With 20.5 nM (active-site concentration) HIV-1 RT, a maximum emission spectrum was centered at 344 nm. The addition of NCp7 resulted in a quenching of the tryptophan fluorescence in a saturable, concentration-dependent manner (Fig. 1a). Therefore, these data indicate that NCp7 is binding to RT. The relative fluorescence at the maximum emission wavelength was determined for the various NCp7 concentrations, and the data were fit to a quadratic equation to provide a K_d of 30 nM for HIV-1 NCp7 binding to HIV-1 RT (Fig. 1b). Additional experiments using size-exclusion membrane filtration and SDS-PAGE gel analysis were conducted to confirm the interaction between RT and NCp7 (see Supporting Information, Supplementary Fig. S6a). Through the use of a 50,000 molecular weight cutoff (MWCO) membrane, NCp7 was retained in the concentrate in the presence of RT as determined by SDS-PAGE gel analysis. Without RT, however, NCp7 was found in the membrane flow through fraction. When heat-annealed or NCp7-facilitated annealed radiolabeled primer–templates were included in the presence RT, they were also retained in the concentrate (Supporting Information, Supplementary Fig. S6b).

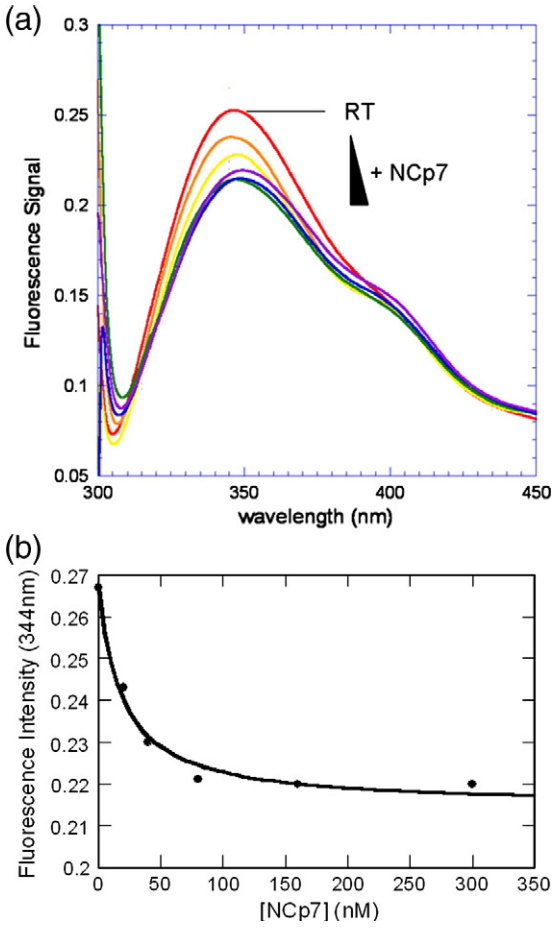

Fig. 1. Examining the direct interaction of HIV-1 RT and HIV-1 NCp7 by fluorescence titration. (a) Fluorescence spectra of HIV-1 RT in the absence and presence of HIV-1 NCp7. Fluorescence emission was recorded for HIV-1 RT (20.5 nM, active-site concentration), shown in red and then with increasing concentration of NCp7 (0–300 nM), 20 nM NCp7 shown in orange, 40 nM NCp7 shown in yellow, 80 nM NCp7 shown in green, 160 nM NCp7 shown in blue and 300 nM NCp7 shown in purple. The excitation was performed at 285 nm. (b) K_d curve of HIV-1 NCp7 to HIV-1 RT. The fluorescence signal at the maximum emissions wavelength was determined for each concentration of NCp7. The fluorescence signal was plotted with NCp7 concentration. The data were fit using the quadratic equation in order to determine the K_d.

Determination of the K_d of DNA to HIV-1 RT with heat-annealed and NCp7-annealed primer–templates

The next step in assessing the effect of NCp7 on reverse transcription was to determine whether the binding affinity of the primer–template to HIV-1 RT was affected. It has been established that RT, NCp7 and viral RNA are packaged together in the virions. Therefore, it is likely that under physiological conditions, RT catalysis would utilize an NCp7-facilitated annealed primer–template. Heat-annealed and NCp7-facilitated annealed DNA/DNA primer–templates were used for these experiments (see Supporting Information, Supplementary Figs. S2a and b for gel analysis used to establish proper annealing). Two different methods were utilized in order to examine the binding of the primer–template to the enzyme.

The intrinsic fluorescence of HIV-1 RT was once again used. With 20.5 nM HIV-1 RT, the fluorescence was measured at a maximal excitation wavelength of 285 nm, and the maximum emission was centered at 344 nm. The addition of the heat-annealed DNA/DNA primer–template resulted in a quenching of tryptophan fluorescence in a saturable and concentration-dependent manner (data not shown). The relative fluorescence at the maximum emission wavelength was determined as a function of primer–template concentrations. These data were fit to a quadratic equation to determine a K_d of <20 nM for the heat-annealed primer–template binding to HIV-1 RT (Fig. 2a). Similar results were obtained for NCp7-facilitated annealed primer–template (Fig. 2b).

Another method to determine the dissociation constant of the RT·DNA complex with the heat-annealed and NCp7-annealed primer–templates is

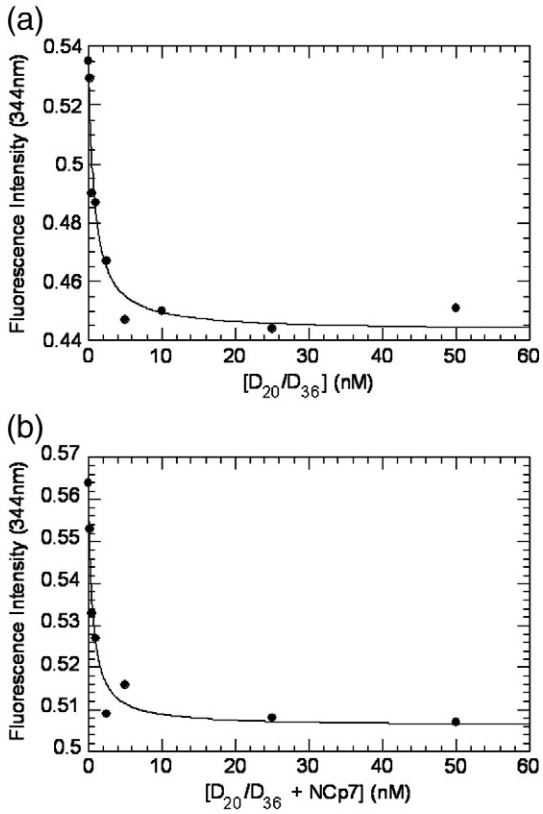

Fig. 2. Determination of K_d of DNA to HIV-1 RT with heat-annealed and NCp7-annealed primer–templates using fluorescence spectroscopy. Fluorescence emission was recorded for HIV-1 RT (20.5 nM, active-site concentration) with increasing concentration of DNA/DNA primer–template. The excitation was performed at 285 nm, and the emission was at a maximum of 344 nm. The fluorescence signal at the maximum emissions wavelength was determined for each concentration of primer–template. The fluorescence signal was plotted with primer–template concentration for the heat-annealed primer–template and the NCp7-annealed primer–template. The data were fit using the quadratic equation in order to determine the K_d. The K_d value for both primer–templates was very tight of <20 nM.

to examine the DNA concentration dependence upon nucleotide product formation during catalysis. The formation of [RT:Primer–Template] *versus* [Primer–Template] was plotted to determine the K_d of DNA binding to HIV-1 RT (Fig. 3). The data were fit to a quadratic equation as previously described.[30] The K_d of DNA to HIV-1 RT with the heat-annealed primer–template is 3.9 nM (●), which agrees with previously performed experiments.[30] The K_d of DNA to HIV-1 RT with the NCp7-facilitated primer–template is 3.3 nM (◊). From the data using these two methods, we can conclude that HIV-1 NCp7 does not affect the binding affinity of the primer–template to HIV-1 RT.

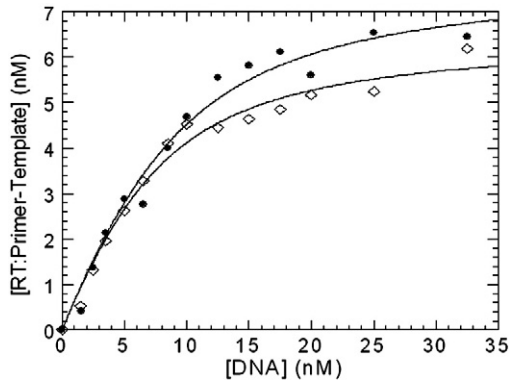

Fig. 3. Determination of K_d of DNA to HIV-1 RT with heat-annealed and NCp7-annealed primer–templates using chemical quench. RT (20 nM) was pre-incubated with increasing concentrations of primer–template and then mixed with 10 mM $MgCl_2$ and 100 μM dCTP, for a reaction time of 250 ms. The curves are a fit of the data to a quadratic equation. For the heat-annealed primer–template, the calculated K_d was 3.9 nM (●). For the NCp7-facilitated annealed primer–template, the calculated K_d was 3.3 nM (◊).

Pre-steady-state kinetics of single-nucleotide incorporation with HIV-1 RT and HIV-1 NCp7-facilitated annealed primer–templates

Previously conducted experiments have been performed to determine the effect of NCp7 on

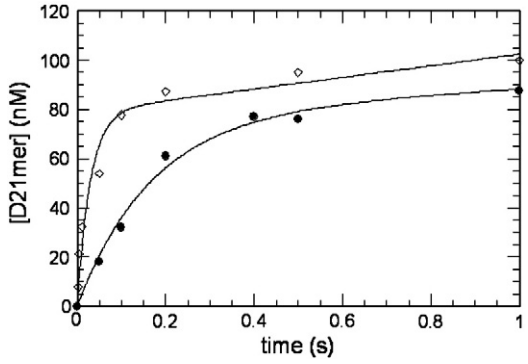

Fig. 4. Pre-steady-state burst kinetics of dCTP incorporation with either heat-annealed (●) or NCp7-facilitated annealed (◊) primer–template. Incorporation of dCTP (100 μM) was performed in the presence of 10 mM $MgCl_2$, mixed with 100 nM RT and 300 nM primer–template in buffer containing 50 mM Tris–HCl, pH 7.8, and 50 mM NaCl at 37 °C. The amount of product formed *versus* time was plotted and then fit to a burst equation as described and the curves as shown. The observed rate for the burst phase was determined for both primer–templates: $k_{obs} = 6 \pm 0.8\ s^{-1}$ for heat annealed and $k_{obs} = 33.7 \pm 9.8\ s^{-1}$ for the NCp7-facilitated annealed primer–template. The linear phase was also examined, k_{ss}, and is approximately 2-fold greater with the NCp7-facilitated annealed primer–template compared to the heat annealed.

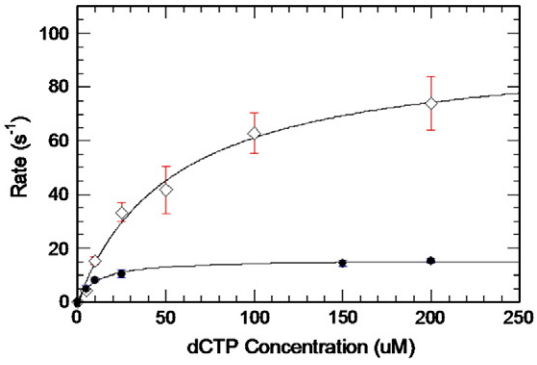

Fig. 5. Determination of k_{pol} and K_d for dCTP incorporation with either heat-annealed or NCp7-facilitated annealed primer–template. The dCTP concentration dependence on the rate of incorporation, k_{obs}, into the primer–template using HIV-1 RT for heat-annealed (●) or NCp7-facilitated annealed (◊) primer–templates was determined. The data were then fit to a hyperbolic equation as described previously. For each data point, all errors are less than 15%.

various steps in reverse transcription.[14,15–18,21,22] These studies have primarily used heat-annealed primer–templates in order to examine strand transfer, processivity and mispriming fidelity to assess the role of NCp7 in modulating the polymerization activities of RT. (+)-DNA strand transfer has been examined using NC-facilitated annealed primer–templates;[10] however, the reaction kinetics for (+)-DNA strand synthesis by RT using NCp7-facilitated annealed primer–templates have not been examined in detail. We speculate that there might be additional roles for NCp7 in modulating RT catalysis. One can utilize pre-steady-state kinetics to address this question. This method allows determination of the maximum rate of incorporation, as well as the binding affinity of the incoming nucleotide to HIV-1 RT during this process.

In order to determine the effects of NCp7 during single-nucleotide incorporation, we used the NCp7-facilitated annealed primer–template and examined the kinetics of deoxycytidine triphosphate (dCTP) and deoxythymidine triphosphate (dTTP) incorporation by HIV-1 RT. With single-nucleotide incorporation, the reaction times are performed on a millisecond timescale. Therefore, we utilized rapid chemical quench methodology to perform reactions in this time domain. Pre-steady-state burst experiments were performed. Under these pseudo-first-order reaction conditions, the DNA substrate is in slight excess of the enzyme (HIV-1 RT) in order to allow an examination of the first enzyme turnover as well as subsequent enzyme turnovers. The reactions were performed as described under Materials and Methods.[35] The resulting data were then fit to a burst equation described by an exponential phase to determine the first-order rate constant for product formation and a linear phase representing the steady-state rate of product release. The first-order rate constant gives the incorporation rate k_{obs}, and the linear phase yields the steady-state rate k_{ss}. Representative data curves for these reactions are shown in Fig. 4. A biphasic burst of product formation is observed from these curves for both the heat-annealed (●) and the NCp7-facilitated annealed (◊) primer–templates. In Fig. 4, the k_{obs} values are 6.0 ± 0.8 s^{-1} for heat-annealed (●) and 33.7 ± 9.8 s^{-1} for the NCp7 -facilitated annealed (◊) primer–templates. It is evident that the NCp7-facilitated annealed primer–template has a much faster rate at this concentration of deoxynucleoside triphosphate (dNTP) compared to the heat-annealed primer–template.

Next, we examined the dNTP concentration dependence on the incorporation rate in order to determine the dissociation constant K_d and the maximum rate of incorporation k_{pol}. It is clear that the K_d curves for the heat-annealed (●) and the NCp7-facilitated annealed (◊) primer–templates are different (Fig. 5), as is evident in the kinetic values shown in Table 1. There is a 3- to 7-fold increase in the rate of dTTP and dCTP incorporation with the NCp7-facilitated annealed primer compared to the heat annealed. However, the binding affinity of the nucleotide is ~2-fold lower with the NCp7-facilitated annealed primer–template. From this data, the efficiency (k_{pol}/K_d) for nucleotide incorporation with HIV-1 RT can be determined as shown in Table 1. The efficiency is slightly enhanced with the NCp7-facilitated annealed primer–template compared to the heat-annealed primer–template.

A closer examination of the earliest time domain was provided by experiments performed under single-turnover conditions. In these reactions, the enzyme is present in 5-fold excess over the primer–template concentration, which allows us to isolate the

Table 1. Kinetic constants for incorporation of dCTP and dTTP by HIV-1 RT with heat-annealed or NCp7-facilitated annealed primer–templates

Primer–template	dNTP	k_{pol} (s^{-1})	K_d (μM)	k_{pol}/K_d (μM^{-1} s^{-1})
DNA/DNA heat annealed	dCTP	15.7 ± 0.4	10.5 ± 1.1	1.5 ± 0.2
DNA/DNA NCp7-facilitated annealed		56.6 ± 4.6	23.5 ± 6.4	2.4 ± 0.6
DNA/DNA heat annealed	dTTP	39.4 ± 2.8	25.7 ± 6.9	1.5 ± 0.4
DNA/DNA NCp7-facilitated annealed		125.4 ± 14.5	66.6 ± 18.2	1.9 ± 0.6

Table 2. Rates of incorporation for single and multiple nucleotides by HIV-1 RT with heat-annealed or NCp7-facilitated annealed primer–templates under single-enzyme turnover conditions

		Single exponential fit	Double exponential fit	
	Primer–template	k_1 (s^{-1})	k_1 (s^{-1})	k_2 (s^{-1})
Single nucleotide	DNA/DNA heat annealed	3.7 ± 0.6	N/A	N/A
	DNA/DNA NCp7-facilitated annealed	28.7 ± 4.5	64.7 ± 14.1	5.3 ± 2.1
Multiple nucleotide	DNA/DNA heat annealed	7.1 ± 0.8	N/A	N/A
	DNA/DNA NCp7-facilitated annealed	33.1 ± 6.8	94.7 ± 12.6	4.2 ± 1

chemical step and observe the first enzymatic turnover by HIV-1 RT. From the k_{obs} values, the rate for single-nucleotide incorporation is almost 8-fold faster for the NCp7-annealed primer–template (28.7 ± 4.5 s^{-1}) compared to the heat-annealed primer–template (3.7 ± 0.6 s^{-1}) (Supporting Information, Supplementary Fig. S3). Also, product formation with the NCp7-annealed primer–template appeared to be biphasic (as illustrated in Supporting Information, Supplementary Fig. S4a). This figure illustrates a fitting of the reaction kinetics with both single and double exponential equations. The double exponential fit provided values of 64.7 ± 14.1 s^{-1} for the fast phase and 5.3 ± 2.1 s^{-1} for the slow phase. The results for single-turnover experiments with single-nucleotide incorporation are summarized in Table 2.

Pre-steady-state kinetics of incorporation with HIV-1 RT in the presence of NCp7 using heat-annealed primer–templates

As mentioned above, previous studies to define the role of NCp7 in various aspects of reverse transcription have been examined in the presence of NCp7 as opposed to NCp7-facilitated annealing.[14,16,36,37] Therefore, we examined whether the difference in kinetics that was observed was due to the simple presence of NCp7. In these experiments, we added NCp7 to the heat-annealed primer–template and performed single-nucleotide incorporation experiments. As seen in Table 3, in the presence of NCp7, there is a slight increase in the rate of incorporation as compared to the absence of the protein. Moreover, the binding affinity does not change with NCp7 in the reaction. From this information, we conclude that the substantial increase in rate and the change in binding affinity are not merely the result of the presence of the protein but in fact due to specifically NCp7- facilitated annealing of the primer–template.

Table 3. Kinetic constants for incorporation of dCTP by HIV-1 RT in the absence or presence of NCp7

Primer–template[a]	k_{pol} (s^{-1})	K_d (μM)
DNA/DNA	15.7 ± 0.4	10.5 ± 1.1
DNA/DNA with NCp7	22.2 ± 0.4	10.5 ± 3.8

[a] Heat-annealed primer–template.

Extension using HIV-1 RT under pre-steady-state conditions with HIV-1 NCp7

Under pre-steady-state conditions, we examined extension using HIV-1 RT and the heat-annealed or NCp7-facilitated annealed primer–template with all four nucleotides present at various time points—from 5 ms to 10 s. Under pseudo-first-order reaction conditions and at millisecond timescale, there is clearly a difference in product formation between the two primer–templates (Fig. 6a). With the NCp7-annealed primer–template, a longer product is observed at 100 ms compared to the heat-annealed primer–template (Fig. 6a, boxed areas). The bands were quantified, and product formation *versus* time was plotted for each of the primer–templates (Fig. 6b). From this graph, we observed that the NCp7-annealed primer–template (◊) has more product formed compared to the heat-annealed primer–template (●). Also, the rate of product formation for the NCp7-annealed primer–template is faster compared to using the heat-annealed primer–template.

We also examined multiple-nucleotide extension of the primer–templates by RT under single-turnover conditions. The difference in product formation between the two different primer–templates is even more evident (Fig. 7a). By 5 ms, RT has extended a substantial amount of the NCp7-annealed primer–template (right), unlike the heat-annealed primer–template (left). Once again, the gels were quantified, and product formation *versus* time was plotted (Fig. 7b). Similar to the reactions under burst conditions, the NCp7-annealed primer–template (◊) has formed more of the product by 100 ms compared to the heat-annealed primer–template (●). Therefore, the NCp7-annealed primer–template facilitates nucleotide extension by RT on millisecond timescale. A closer look at the reaction kinetics for multiple-nucleotide extension for the NCp7-annealed primer–template by RT also reveals biphasic product formation (Supporting Information, Supplementary Fig. S4b), similar to what was observed with single-nucleotide incorporation. The observed rates for the single-turnover data using single and double exponential equations were determined as shown in Table 2.

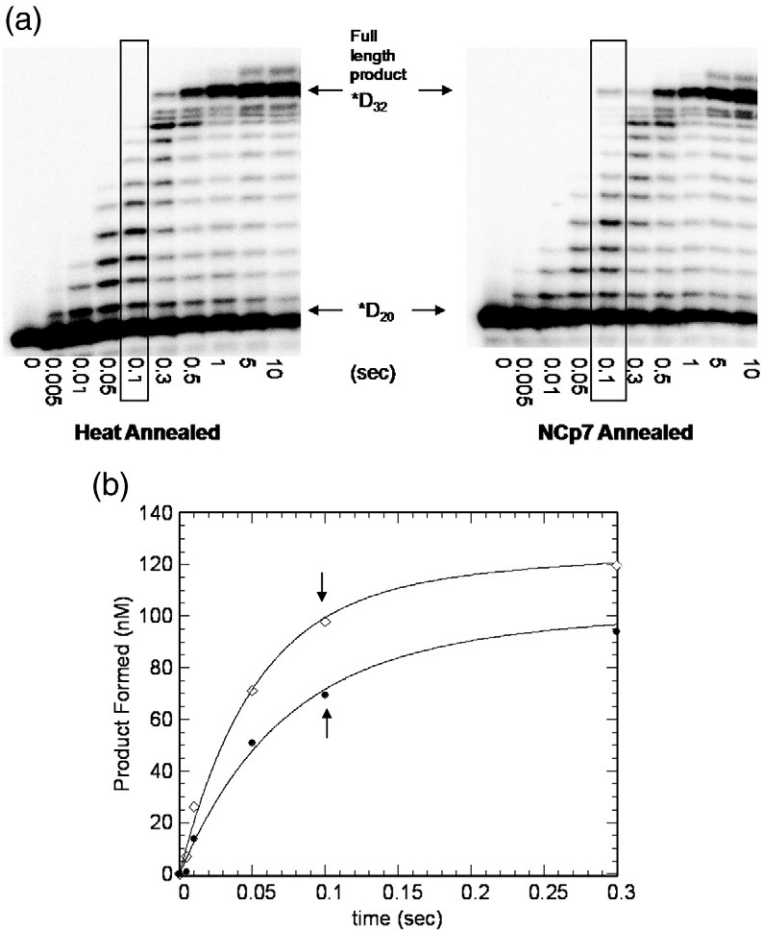

Fig. 6. Examining extension of heat-annealed or NCp7-facilitated annealed primer–templates using HIV-1 RT under pre-steady-state pseudo-first-order conditions. Experiments in the presence of all four dNTPs (100 μM) with 10 mM $MgCl_2$, mixed with 100 nM RT and 300 nM primer–template in buffer containing 50 mM Tris–HCl, pH 7.8, and 50 mM NaCl, were performed. (a) Extension of the two primer–templates by RT was observed. There is a longer product formed at the 0.1-s time point with the NCp7-annealed primer–template compared to the heat-annealed primer–template. (b) The amount of product formed by extension *versus* time was plotted for both primer–templates. The NCp7-facilitated annealed primer–template (◊) has more product formed at each time point and at a faster rate compared to the heat-annealed primer–template (●). Arrows are pointed to the amount of product formed for each primer–template at the 0.1-s time point. There is more product formed with the NCp7-facilitated annealed primer–template compared to the heat-annealed primer–template.

Examining the requirements for NCp7 rate enhancement of DNA synthesis by RT

From the above results, we decided to examine which aspects of NCp7 mediated interactions that are required for facilitated annealing as well as for the enhancement of DNA-directed synthesis by HIV-1 RT. In order to examine the importance of the NCp7 zinc finger and N-terminal domain of NCp7 interactions, we disrupted these in a stepwise manner by examining four different preparations of NCp7 (designated by color coding, Supplementary Fig. 7): native, untreated NCp7 (blue); NCp7 treated with 100 mM ethylenediaminetetraacetic acid (EDTA) (green); NCp7 in high salt, 500 mM NaCl (purple); and EDTA-treated NCp7 in the presence of high salt (yellow). We examined the rate of single-nucleotide incorporation under single-turnover conditions using 200 μM dCTP and the forms of NCp7 described above. As controls, we determined the rate of incorporation using the native NCp7-facilitated annealed primer–template (blue **1**), in the presence of the native NCp7 using a heat-annealed primer–template (blue **2**) and in the absence of NCp7 (red **3**).

As previously mentioned, the NCp7 purified from *Escherichia coli* contains two zinc ions as determined by ESI-TOF MS. The zinc ions were chelated by treating the protein with 100 mM EDTA and omission of zinc to buffers in any the following reactions. The absence of zinc in the NCp7 was confirmed by ESI-TOF MS (data not shown). The protein was used for facilitated annealing of the primer–template and subsequently single-nucleotide incorporation by HIV-1 RT (green **4**). The rate of product formation was similar to that of reactions in the presence of the native NCp7 using a heat-annealed primer–template. Next, we examined whether the presence of this zinc-free form of NCp7 is able to enhance RT activity. Using a heat-annealed primer–template, we performed single-nucleotide incorporation experiments with an equivalent amount of the EDTA-treated NCp7. In the presence of the zinc-free NCp7, we observed a 2-fold increase in the rate of single-nucleotide incorporation (green **5**), similar to what was observed with the zinc-free NCp7-facilitated annealed primer–template conditions. From these data, we can conclude that the zinc ions are required for a productive form of an NCp7-facilitated annealed

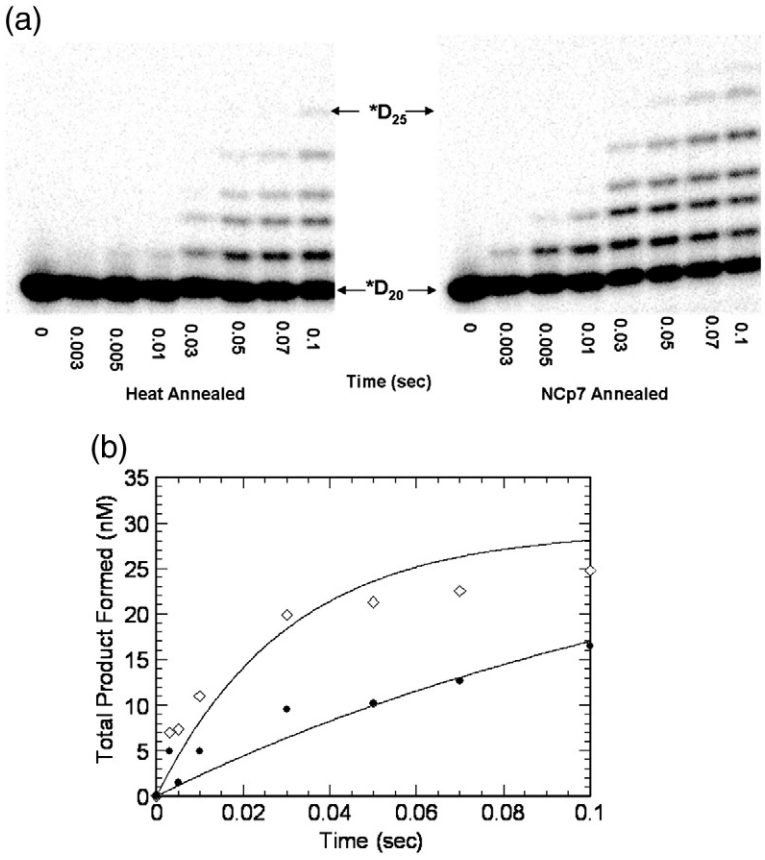

Fig. 7. Examining extension of heat-annealed or NCp7-facilitated annealed primer–templates using HIV-1 RT under pre-steady-state single-turnover conditions. Experiments in the presence of all four dNTPs (100 μM) with 10 mM $MgCl_2$, mixed with 250 nM RT and 50 nM primer–template in buffer containing 50 mM Tris–HCl, pH 7.8, and 50 mM NaCl, were performed. (a) Extension of the two primer–templates by RT was observed. A longer product is formed faster at the early millisecond time points with the NCp7-annealed primer–template compared to the heat-annealed primer–template. (b) The amount of product formed by extension *versus* time was plotted for both primer–templates. The NCp7-facilitated annealed primer–template (◊) has more product formed at each time point and at a faster rate compared to the heat-annealed primer–template (●).

primer–template; however, they are not required for a productive form of the NCp7–RT complex to enhance reverse transcription.

The requirement for interactions with the basic residues present in the N-terminal region of NCp7 was also examined. The NCp7 was present in a buffer containing high salt (500 mM NaCl) in order to disrupt these interactions. The NCp7-facilitated annealing of the primer–template was prepared under high salt conditions as well. Single-nucleotide incorporation was performed with this primer–template, and the rate was slightly increased (purple **6**), similarly to the native protein's presence reaction. Thus, the N-terminal region is also important for making a productive NCp7-facilitated annealed primer–template for single-nucleotide incorporation by RT.

The zinc fingers as well as the N-terminal residues of NCp7 were disrupted by treatment with EDTA and present in a high salt buffer. NCp7-facilitated annealing of the primer–template was attempted, but a higher-molecular-weight primer–template was not formed (Supplementary Fig. 2c). This primer–template migrated on a non-denaturing gel similarly to a heat-annealed primer–template, thus indicating that the interactions with the zinc fingers and the N-terminal basic residues are necessary for a nucleoprotein complex. The rate of single-nucleotide incorporation was slightly higher compared to that of the heat-annealed primer–template (yellow **7**). These data reveal that the lack of the zinc ions and the disruption of the interactions in the N-terminal residues affect facilitated annealing of the primer–template; however, they are not necessary for the interaction of NCp7 and HIV-1 RT.

NCp7 increases the fidelity of HIV-1 RT

Previous work has demonstrated improved fidelity of reverse transcription by NCp7 by inhibition of mispriming during (+)-strand synthesis.[21,22] Using pre-steady-state kinetics and the NCp7-facilitated annealed primer–template, we examined the ability of HIV-1 RT to incorporate an incorrect nucleotide. In order to examine the fidelity of HIV-1 RT, we utilized a primer–template in which dCTP is the correct nucleotide and performed misincorporation studies with dTTP to emulate a purine–pyrimidine mismatch.

At the same timescale, there is more product formed with the heat-annealed primer–template compared to the NCp7-facilitated annealed primer–template (Fig. 8). Quantitation of these data allowed us to determine the rate of incorporation by RT (k_{pol}), the binding affinity of the incorrect nucleotide (K_d)

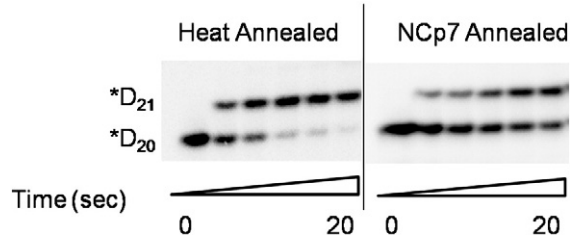

Fig. 8. Misincorporation of a single nucleotide using either heat-annealed or NCp7-facilitated annealed primer–template. Incorporation of an incorrect nucleotide (2 mM dTTP) and 10 mM $MgCl_2$, mixed with 250 nM RT and 50 nM primer–template in buffer containing 50 mM Tris–HCl, pH 7.8, and 50 mM NaCl was performed at various time points. Nucleotide incorporation is complete by 20 s with the heat-annealed primer–template. Through the use of the NCp7-facilitated annealed primer–template, 50% of the product has been formed at the final time point shown.

and the efficiency of incorporation (k_{pol}/K_d). In addition, we determined the fidelity of the enzyme ($[(k_{pol}/K_d)_{correct} + (k_{pol}/K_d)_{incorrect}]/(k_{pol}/K_d)_{incorrect}$), as shown in Table 4. The rate of incorporation of the incorrect nucleotide is 2-fold slower with the NCp7-facilitated annealed primer–template compared to that of the heat-annealed primer–template. However, the binding affinity is unchanged. Therefore, the efficiency of misincorporation by RT is almost 2-fold less with the NCp7-facilitated annealed primer–template. Calculating the efficiency of incorporation of the correct and incorrect nucleotides allowed us to determine the fidelity of the RT using these two primer–templates. The polymerase had a higher fidelity (3-fold) using the NCp7-annealed primer–template compared to the heat annealed. These data extend our understanding and suggest another mechanism of NCp7 in enhancing HIV-1 RT, by increasing the fidelity for the polymerase during single-nucleotide incorporation.

Discussion

HIV-1 NCp is essential for viral replication, and its role in reverse transcription has been the focus of many recent studies. This nucleic acid binding protein has been shown to facilitate the annealing of DNA and RNA primer and template strands,[7,8,10] enhance strand transfer and processivity during reverse transcription[10,14–16] and prevent mispriming during (+)-strand synthesis.[21,22] However, details of the molecular mechanisms by which NCp7 may modulate DNA-directed polymerization at the enzymatic level of HIV-1 RT are still being elucidated. Many mechanistic studies evaluating the role of NCp7 on RT polymerization have used heat-annealed primer–templates in the presence of NCp7. The goals of the current study were to characterize and quantitate the interaction of RT and NCp7 as well as examine DNA-directed polymerization catalyzed by RT using DNA/DNA primer–templates based upon the (+) PBS proviral DNA sequence prepared by NCp7-facilitated annealing. This analysis was carried out using a combination of equilibrium fluorescence and pre-steady-state kinetics, allowing us to delineate the effects of NCp7 on reverse transcription by RT during (+)-DNA strand synthesis.

Equilibrium fluorescence titration experiments demonstrated that, in the presence of NCp7, a saturable, concentration-dependent quenching of fluorescence of the RT (Fig. 2a) was observed, and the two proteins directly interact with a very tight binding affinity, 30 nM (Fig. 2b). This NCp7–RT complex has been previously identified, and the protein–protein interactions have been shown to occur through the conserved structure of the zinc finger domains.[28,29] Our results are in accord with earlier studies that suggested a submicromolar affinity using immobilized resin and Western blotting.[29] This tight NCp7–RT interaction indicates the possibility of NCp7 affecting the process of reverse transcription. Having shown the tight nanomolar interaction between NCp7 and RT, related experiments examined whether the NCp7-facilitated annealed DNA/DNA primer–template has a different binding affinity for the enzyme as compared with heat-annealed primer–template. Through the use of two different methods, fluorescence and incorporation by RT, our results indicate that there is no difference in the binding affinity of the standard heat-annealed *versus* the NCp7-facilitated annealed primer–templates to RT (Figs. 2 and 3). Therefore, NCp7 does not alter the binding affinity of the primer–template to the RT.

There are many discrete steps involved in the process of reverse transcription to convert the viral RNA genome into the double-stranded viral DNA before integration into the host cell genome.

Table 4. Kinetic constants for misincorporation of dTTP by HIV-1 RT with heat-annealed or NCp7-facilitated annealed primer–templates

Primer–template	k_{pol} (s^{-1})	K_d (μM)	k_{pol}/K_d ($\mu M^{-1}\ s^{-1}$)	Fidelity[a]
DNA/DNA heat annealed	0.26 ± 0.02	404 ± 133	6.5×10^{-4}	2308
DNA/DNA NCp7-facilitated annealed	0.15 ± 0.01	394 ± 101	3.8×10^{-4}	6316

[a] Calculated using the following equation: $[(k_{pol}/K_d)_{correct} + (k_{pol}/K_d)_{incorrect}]/(k_{pol}/K_d)_{incorrect}$.

However, the role of nucleocapsid-annealed primer–templates on single-nucleotide incorporation has yet to be studied in detail. When examining the rate of nucleotide incorporation using steady-state kinetics, one observes the slowest rate of the reaction, which in the case of RT is the dissociation of the elongated primer–template and the enzyme. Pre-steady-state kinetics provide a direct measurement of the incorporation rate, providing a more precise means of examining chemical catalysis.[30] Thus, these events occur at the active site of RT. In order to examine (+)-strand synthesis, we utilized a DNA/DNA primer–template that contains PBS(+) and PBS (−). The pre-steady-state pseudo-first-order experiments performed with heat-annealed and NCp7-facilitated annealed primer–templates clearly reveal that the kinetics with the NCp7-facilitated annealed primer–template are different from those of the heat-annealed primer–template (Figs. 4–7). This difference is not nucleotide specific and was observed with both dCTP and dTTP (Table 1).

In our study, the k_{pol} for nucleotide incorporation by RT for facilitated annealed primer–template substrate is 3- to 7-fold faster relative to heat annealed in the absence of NCp7. The effect on k_{pol} is somewhat offset by a 2-fold weaker K_d for nucleotide binding with the facilitated annealed substrate relative to heat annealed; however, this still leads to a 1.6-fold overall net increase in incorporation efficiency. While this increase in efficiency may be small when dNTP concentrations are in the range of the K_d, at saturating concentrations of dNTP in the cell that have been estimated to be in the 100- to 200-μM range,[38,39] the rate of nucleotide incorporation with the facilitated annealed primer–template substrate would be 3- to 7-fold faster. Accordingly, at cellular concentrations of dNTPs, one would expect that there would be significant impact on function with the NCp7-facilitated annealed primer–template during (+)-DNA-directed synthesis of the viral genome.

This nucleotide rate enhancement by the NCp7-annealed primer–template is also observed during the process of multiple-nucleotide extension (Figs. 6 and 7). Pre-steady-state pseudo-first-order experiments and single-turnover experiments reveal that RT utilizing the NCp7-facilitated annealed primer–template catalyzed a more elongated product at a faster rate compared to heat-annealed primer–template (Figs. 6b and 7b). This enhanced extension with NCp7-facilitated annealed primer–template during (+)-DNA strand synthesis occurring in later steps of viral DNA synthesis is consistent with previous studies examining the earlier initiation step of reverse transcription involving tRNA.[24] This increase in the rate of incorporation by the NCp7-annealed primer–template was observed in the process of extension, especially under single-turnover conditions.

Single-turnover experiments with the NCp7-annealed DNA/DNA primer–template demonstrated biphasic kinetics with single-nucleotide incorporation and extension by RT (Fig. S4, Supporting Information). One plausible explanation for the biphasic kinetics with the NC-facilitated annealed substrate would be two distinct populations due to the presence of DNA nucleotide substrate in two different conformations. Additional experiments performed with the NCp7-annealed primer–template using native gel analysis show that the nucleoprotein complex migrated in a super shift relative to the heat-annealed primer–template (Fig. S2b, Supporting Information). This analysis also revealed that, occasionally, a small amount of this primer–template migrates at a position equivalent to that observed with the heat-annealed form (14%) and may be the source of the slower phase of the biphasic kinetic behavior.

The chaperone activity of NCp7 has been extensively studied.[13,40,41] NCp7 chaperones the annealing of primer tRNA to PBS for initiation and nascent 5′ long terminal repeat DNA to 3′ long terminal repeat HIV RNA.[42–44] The presence of NCp7 has been shown to accelerate the annealing reaction 3000-fold[7] caused by the protein's ability to destabilize the primer and template sequences and activate the intermolecular annealing. With this information, we decided to utilize NCp7's chaperone activity by making NCp7-facilitated annealed primer–templates. However, there have been a number of groups that examined NCp7 and the process of reverse transcription using the presence of the protein instead of NCp7-facilitated annealed primer–templates. This leads us to address if the results we observed for single-nucleotide incorporation are merely due to presence of NCp7 *versus* specifically NCp7-facilitated annealing of the primer–template. In these experiments, we examined the rate of incorporation for heat-annealed primer–template in the presence of NCp7 with an NC-to-nucleotide ratio of 1:7, which is equivalent to the amount present in facilitated annealing. We observed that the k_{pol} was slightly increased, which may indicate that the presence of NCp7, perhaps through its interaction with RT, enhances single-nucleotide incorporation. This information corresponds to previously published results on the enhancement of NCp7 on RT.[14–16] Also observed was the lack of change in the K_d of the next incoming nucleotide, which indicates that the NCp7-annealed primer–template is in a different conformation compared to the heat-annealed primer–template, therefore affecting the binding affinity. In the presence of much higher concentrations of NCp7, the rate of nucleotide incorporation was dramatically slower (see Fig. S5, Supporting Information) as has been observed previously by Grohmann *et al.*[19] Therefore, the large increase in k_{pol} and change in K_d

are due not just to the presence of the protein but also to NCp7-facilitated annealing of the primer–template. Although the process of reverse transcription can occur with the heat-annealed primer–template, the facilitated annealed primer–template might be considered more physiologically relevant.

The zinc fingers and also the N-terminal domain of NCp7 have been shown to be responsible for the direct interaction between the protein and RT.[28,29] DNA destabilizing activity as well as the annealing activity of NCp7 is lost when the N-terminal domain or the zinc ions are not present.[45] Single-nucleotide incorporation experiments using NCp7 treated with EDTA for facilitated annealing of the primer–template as well as in the presence of the zinc-free protein with a heat-annealed primer–template show a slight enhancement in the rate of product formation. Therefore, these results indicate that although the zinc ions are necessary for proper nucleotide binding with the primer–templates, they are not required for interaction with HIV-1 RT. Disruption of the interaction between the N-terminal residues and the nucleic acids in the presence of high salt demonstrated a slight increase in the rate of incorporation, similar to the EDTA-treated NCp7. However, disruption of both the N-terminal residues and the zinc fingers of NCp7 disables the protein's ability to facilitate annealing of the primer–template and form a nucleoprotein complex (Supplementary Fig. 2c). These results are in agreement with a previous study by Cruceanu *et al*. who observed that, upon examination of the NCp7 and DNA interactions using an N-terminal truncation mutant that was treated with EDTA, the kinetics were very similar to those obtained in the absence of the protein.[45] Single-nucleotide incorporation experiments revealed that this protein does slightly increase the rate of incorporation, perhaps through an interaction with HIV-1 RT. Our data suggest the requirement of the N-terminal region and the presence of zinc for interaction with nucleic acids for NCp7-facilitated annealing of the primer–template and its enhancement of RT.

Altogether, these data suggest that it is important to chelate the ions from the zinc fingers as well as interrupt the interactions with the N-terminal region of NCp7, in order to disrupt the interaction of the protein to the primer and template strands. A recent review by Darlix *et al*. discussed the determinants that may govern NCp7 binding affinity for various oligonucleotides.[46] The binding affinity is affected by salt conditions, oligonucleotide length and sequence. The binding affinities from previously published studies range from 20 nM to 1 μM. Recent works by several groups have shown successful disruption of specific NCp7–nucleic acid interactions. Druillennec *et al*. demonstrated that a hexapeptide mimic of NCp7 has antiviral effects by competing with NCp7 and inhibiting annealing activities and affecting reverse transcription.[47] Similar results have also been obtained by using small molecules. Miller Jenkins *et al*. showed that a series of 2-mercaptobenzamide thioesters affects the zinc finger motif in NCp7 and thus inhibits viral replication. These compounds represent a new class of inhibitors that work as zinc ejectors by reacting with the second zinc finger of NCp7.[48]

Previous studies have demonstrated the ability of NCp7 to affect the fidelity of reverse transcription by prevention of mispriming during (+)-strand synthesis.[21,22] HIV-1 RT is prone to misincorporation of nucleotides due to the lack of proofreading activity. Using pre-steady-state kinetics, we examined the fidelity of the polymerase by determining the kinetic parameters of incorporation of an incorrect nucleotide using a heat-annealed primer–template and an NCp7-facilitated annealed primer–template. From these experiments, we observed that the NCp7 affects fidelity of the enzyme (Fig. 8 and Table 4), by decreasing the rate of incorporation of the incorrect nucleotide and thus increasing RT's fidelity by 3-fold compared to the heat-annealed primer–template. These data suggest that the coating of the primer–template by NCp7 enhances the polymerase's ability to discriminate and have a preference for the correct nucleotide. At a cellular level, it might be expected that increased fidelity of HIV-1 RT provided by the NCp7-annealed primer–templates would allow for increased viral fitness.

From these data, we hypothesize that there are a few possibilities as to how NCp7 is affecting reverse transcription, as illustrated in Fig. 9. Based on previously published data, as well as our single-nucleotide incorporation experiments, the presence of NCp7 enhances reverse transcription. Therefore, the direct interaction between the two proteins may cause a conformational change in RT. On the other hand, our data with the NCp7-facilitated annealed DNA/DNA primer–template suggest that this nucleic acid binding protein may provide a distinct conformation such that this primer–template is in a pre-productive orientation allowing for faster nucleotide incorporation. This nucleoprotein complex may also change the conformation of the enzyme itself to allow for faster catalysis by HIV-1 RT. HIV-1 RT is a flexible polymerase that may accommodate the presence of a small protein such as NCp7. Structural data have given insight into the interactions between NCp7 and RNA and DNA oligonucleotides.[49–51] However, additional structural data on the interaction of RT with NCp7-annealed primer–template would perhaps offer more insight to understand the structural basis of enhanced catalysis.

There are multiple roles present for NCp7 during viral replication—RNA packaging, viral assembly, integration and during reverse transcription.[1,9,13,20,40] This work demonstrates the ability of NCp7 to act as a chaperone in its ability to facilitate annealing, a

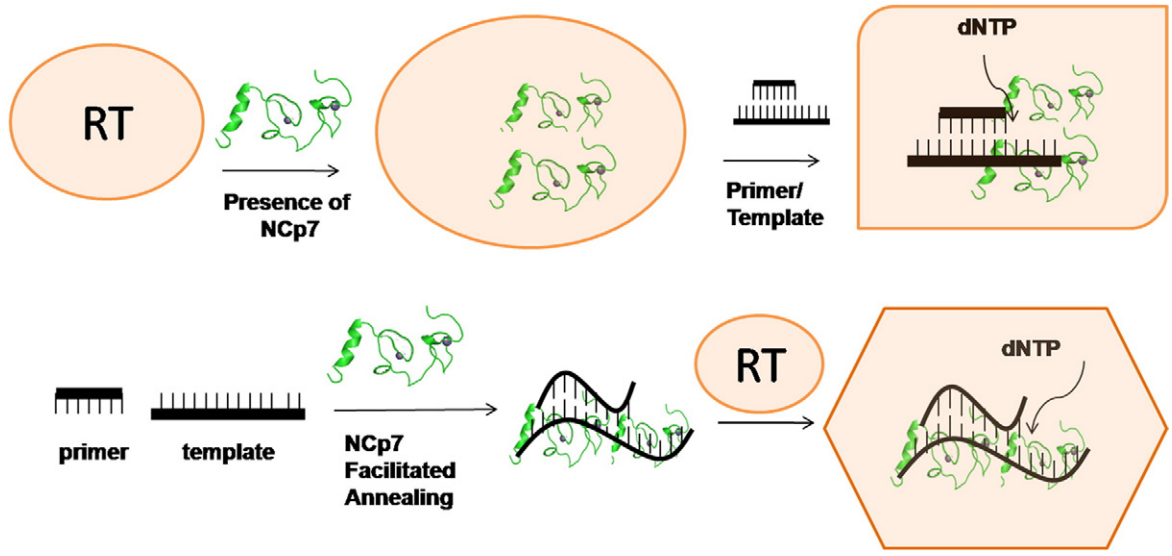

Fig. 9. Mechanisms of NCp7 enhancing reverse transcription. Image of NCp7 created from the NMR structure of the NCp7 and SL3 psi-RNA (PDB: 1A1T). In the presence of NCp7, HIV-1 RT changes conformation upon binding of the protein and primer–template. NCp7-faciliated annealing changes the conformation of the double-stranded primer–template. The binding of this primer–template also changes the conformation of RT to a more productive conformation to allow for faster catalysis.

modulator in enhancing the rate of nucleotide incorporation, and to enhance the fidelity of the error-prone RT. In conclusion, this study demonstrates a positive role for NCp7 in facilitating (+)-DNA strand synthesis during reverse transcription through its interaction with the primer and template, which offers another avenue to exploit as a possible drug target for anti-HIV-1 therapy.

Materials and Methods

Materials

Recombinant HIV-1 RT (p66/p51 heterodimer) clone was kindly provided by Dr. Stephen Hughes and Dr. Andrea Ferris (Frederick Cancer Research and Development Center, MD). The glycerol stock of *E. coli* transformed with HIV-1 NCp7 was provided by Charles McHenry. DNA oligonucleotides that were used as primer and templates for incorporation and extension experiments were synthesized at the Keck Facility at Yale University and purified by 20% polyacrylamide denaturing gel electrophoresis. The sequences of the primers and templates used in this study contain the PBS(−) and PBS(+) sequences: D20 (5′-TCAGGTCCCTGTTCGGGCGC-3′), D23 (5′-TCAGGTCCCTGTTCGGGCGCCAC-3′) and D36 (5′-TCTCTAGCAGTGGCGCCCGAACAGGGACCTGAAAGC-3′). dTTP and dCTP were obtained from GE/Amersham Biosciences.

Purification of HIV-1 RT

Recombinant HIV-1 RT (p66/p51 heterodimer) clone was kindly provided by Dr. Stephen Hughes and Dr. Andrea Ferris (Frederick Cancer Research and Development Center). The C-terminal histidine-tagged RT was purified as previously described with modifications.[52] A cobalt affinity column in the presence of Buffer A with 5 mM imidazole and without Triton was used, and the protein was eluted in the presence of 0.5 M imidazole. The RT was then applied to a Q Sepharose column as previously described, using a linear gradient of 0–1 M NaCl. The protein was stored in a buffer containing 50 mM Tris (pH 7.8), 50 mM NaCl, 2 mM DTT and 10% glycerol. The protein purity as judged by SDS-PAGE analysis with Coomassie staining was >90%.

Purification and analysis of NCp7

The protocol was adapted as previously described.[31] *E. coli* was grown in LB media with 50 μg/ml ampicillin and then induced with a final concentration of 1 mM IPTG at 37 °C. The cells were harvested and then resuspended with an equal weight of 50 mM Tris–HCl, pH 7.5, and 10% sucrose. The frozen cells were resuspended with lysis buffer[31] and sonicated. The cells were then centrifuged for 1 h at 15,000*g*. Polyethyleneimine was added to the supernatant to a final concentration of 0.5% with constant stirring for 15 min. The solution was then centrifuged for 20 min at 10,000*g*. Two ammonium sulfate precipitations were performed to the supernatant, at 40% and then 80%; the solution was centrifuged for 20 min at 10,000*g*. The final pellet was resuspended with 1/5 of the volume from the supernatant after the first centrifugation, with buffer.[31] The solution was dialyzed overnight as previously described.[31] The solution was then applied to a Q Sepharose column, dialyzed and then applied to an SP-Sepharose column, as previously described. The protein was applied to a G-50 Gel Filtration column. The protein was visualized on 17.5% SDS-PAGE gels after each column and judged to be >90% pure.

The purified NCp7 was also analyzed using ESI mass spectroscopy, which was recorded with an Ettan ESI-TOF mass spectrometer (Amersham Biosciences), after buffer exchange in 50 mM ammonium bicarbonate, pH 8, and shown to have two zinc ions bound (Fig. S1).

NCp7 in the absence of zinc was prepared by treating the protein with 100 mM (final) EDTA for 1 h at room temperature. Biospin columns from Bio-Rad were used for buffer exchange for the treated protein, in 50 mM Tris–HCl, pH 7.8, and 50 mM NaCl. The treated NCp7 was analyzed by ESI-TOF MS to examine that the zinc ions were no longer present with the protein. NCp7 was also present in high salt, which contained 50 mM Tris–HCl, pH 7.8, and 500 mM NaCl.

In order to avoid degradation and/or loss of the NC activity, as observed by other laboratories as well as ours,[14] we used the protein within 3 months after purification.

Labeling and annealing of oligonucleotides

Primers for the reverse transcription reactions were 5′-^{32}P labeled with T4 polynucleotide kinase (New England Biolabs) as previously described.[30] [γ-^{32}P]ATP was purchased from GE/Amersham Biosciences. Biospin columns for removal of excess [γ-^{32}P]ATP were purchased from Bio-Rad. All annealing experiments were performed using buffer containing 50 mM Tris–HCl, pH 7.8, and 50 mM NaCl. All primer–templates were annealed using a primer concentration of 1 μM and a template concentration of 1.5 μM, to ensure complete annealing of the primer. The heat-annealed primer–templates were formed by incubation at 90 °C for 5 min, 55 °C for 15 min and then on ice for 15 min. The NCp7-facilitated annealing was performed using the same concentrations as the heat-annealed primer–templates, and 7.5 μM NCp7 was added, which is equivalent to seven nucleotides per NCp7 (based upon a nucleotide 36-mer template, the ratio of 5:1 for [NCp7]:[template]),[24] and incubated at 37 °C for 15 min.

To visualize successful annealing, we analyzed samples of the primer alone and annealed primer–templates by non-denaturing electrophoresis (15%) using SDS-PAGE running buffer. SDS-PAGE running buffer was used to ensure that the complex could be visualized and go into the gel (Fig. S2a of Supporting Information). However, to make sure that NCp7 is present in the NCp7-facilitated annealed primer–template, we also used standard Tris–boric acid–EDTA running buffer (Fig. S2b of Supporting Information).

Direct protein binding experiments with HIV-1 NCp7 and HIV-1 RT

Equilibrium fluorescence measurements were performed using an SLM 4800C spectrofluorometer (Urbana, IL). RT [20.5 nM (active-site concentration)] was diluted in buffer containing 50 mM Tris–HCl, pH 7.8, and 50 mM NaCl in a total volume of 2 ml. The fluorescence of the tryptophan residues in HIV-1 RT was measured at an excitation wavelength of 285 nm with an emissions spectrum ranging from 300 to 500 nm at 1-nm increments. NCp7 (0–300 nM) was added to the RT and incubated for 5 min before each reading. The data were then accumulated and plotted using KaleidaGraph. The binding constant (K_d) was determined by plotting the relative fluorescence *versus* NCp7 concentration, and the data were fit to a quadratic equation, as previously described.[52,53] All experiments were performed at room temperature.

Filtration experiments using a 50,000 MWCO Centricon Ultracel YM-50 centrifugal filter were performed to observe the formation of the HIV-1 NCp7 and HIV-1 RT complex. Amicon Ultra 50,000 MWCO filters were also used to examine the interactions of HIV-1 RT with heat-annealed and NCp7-annealed primer–templates. (Supporting Information Fig. 6)

Pre-steady-state kinetics experiments

Rapid chemical quench experiments were performed as previously described with a KinTek Instrument model RQF-3 rapid quench-flow apparatus.[52] A pre-steady-state kinetic analysis was used to examine the incorporation of dCTP or dTTP using a heat-annealed or NCp7-facilitated annealed DNA/DNA primer–template. The primer–template and HIV-1 RT were pre-incubated on ice for 5 min before loading onto the quench apparatus. For experiments performed with heat-annealed primer–template but in the presence of NCp7, 2.25 μM NCp7 (equivalent concentration present with the NCp7-facilitated annealed primer–template) was added before incubation with HIV-1 RT. K_d determination of the primer–template to RT experiments was carried out at a final concentration of 20 nM HIV-1 RT (total protein concentration), varying concentrations of 5′-labeled primer–template, 10 mM $MgCl_2$ and 100 μM dCTP in the presence of 50 mM NaCl and 50 mM Tris–HCl, pH 7.8 and 37 °C. Pre-steady-state burst experiments were carried out at a final concentration of 100 nM HIV-1 RT (active-site concentration), 300 nM 5′-labeled primer–template, 10 mM $MgCl_2$ and varying concentrations of dNTP in the presence of 50 mM NaCl and 50 mM Tris–HCl, pH 7.8 and 37 °C. The reactions were quenched at various time points by the addition of 0.3 M EDTA. In experiments examining multiple extensions, all four dNTPs were present in the reaction at a concentration of 100 μM. Experiments that examined the fidelity of HIV-1 RT used a primer–template for dCTP incorporation and various concentrations of dTTP. The products were analyzed on a 20% polyacrylamide 8 M urea gel. The products and substrates were quantitated on a Bio-Rad Molecular Imager FX. The data for the K_d determination of RT and primer–template complex were fit to a quadratic equation, as previously described.[30] The data for the single-nucleotide incorporation and extension experiments were fit to a burst equation, as previously described, and the concentration dependence of the burst rate was fit as previously described.[52] These analyses enabled us to determine the maximum rate of dNTP incorporation, k_{pol}, and the equilibrium dissociation constant for the dNTP, K_d.[30]

Acknowledgements

We would like to thank Dr. Stephen Hughes, Dr. Paul Boyer and Dr. Andrea Ferris (National

Institutes of Health) for the HIV-1 RT^{WT} clone and Dr. Charles McHenry (University of Colorado at Boulder) for the NCp7 clone. This work was supported by National Institutes of Health GM 49551 to K.S.A.

Supplementary Data

Supplementary data to this article can be found online at doi:10.1016/j.jmb.2011.12.034

References

1. Darlix, J. L., Garrido, J. L., Morellet, N., Mely, Y. & de Rocquigny, H. (2007). Properties, functions, and drug targeting of the multifunctional nucleocapsid protein of the human immunodeficiency virus. *Adv. Pharmacol.* **55**, 299–346.
2. Haseltine, W. A. (1991). Molecular biology of the human immunodeficiency virus type 1. *FASEB J.* **5**, 2349–2360.
3. Gorelick, R. J., Chabot, D. J., Rein, A., Henderson, L. E. & Arthur, L. O. (1993). The two zinc fingers in the human immunodeficiency virus type 1 nucleocapsid protein are not functionally equivalent. *J. Virol.* **67**, 4027–4036.
4. Sakaguchi, K., Zambrano, N., Baldwin, E. T., Shapiro, B. A., Erickson, J. W., Omichinski, J. G. *et al.* (1993). Identification of a binding site for the human immunodeficiency virus type 1 nucleocapsid protein. *Proc. Natl Acad. Sci. USA*, **90**, 5219–5223.
5. South, T. L., Blake, P. R., Hare, D. R. & Summers, M. F. (1991). C-terminal retroviral-type zinc finger domain from the HIV-1 nucleocapsid protein is structurally similar to the N-terminal zinc finger domain. *Biochemistry*, **30**, 6342–6349.
6. Houzet, L., Morichaud, Z., Didierlaurent, L., Muriaux, D., Darlix, J. L. & Mougel, M. (2008). Nucleocapsid mutations turn HIV-1 into a DNA-containing virus. *Nucleic Acids Res.* **36**, 2311–2319.
7. You, J. C. & McHenry, C. S. (1994). Human immunodeficiency virus nucleocapsid protein accelerates strand transfer of the terminally redundant sequences involved in reverse transcription. *J. Biol. Chem.* **269**, 31491–31495.
8. Remy, E., de Rocquigny, H., Petitjean, P., Muriaux, D., Theilleux, V., Paoletti, J. & Roques, B. P. (1998). The annealing of tRNA3Lys to human immunodeficiency virus type 1 primer binding site is critically dependent on the NCp7 zinc fingers structure. *J. Biol. Chem.* **273**, 4819–4822.
9. Levin, J. G., Guo, J., Rouzina, I. & Musier-Forsyth, K. (2005). Nucleic acid chaperone activity of HIV-1 nucleocapsid protein: critical role in reverse transcription and molecular mechanism. *Prog. Nucleic Acid Res. Mol. Biol.* **80**, 217–286.
10. Auxilien, S., Keith, G., Le Grice, S. F. & Darlix, J. L. (1999). Role of post-transcriptional modifications of primer tRNALys,3 in the fidelity and efficacy of plus strand DNA transfer during HIV-1 reverse transcription. *J. Biol. Chem.* **274**, 4412–4420.
11. Bampi, C., Jacquenet, S., Lener, D., Decimo, D. & Darlix, J. L. (2004). The chaperoning and assistance roles of the HIV-1 nucleocapsid protein in proviral DNA synthesis and maintenance. *Int. J. Biochem. Cell Biol.* **36**, 1668–1686.
12. Thomas, J. A. & Gorelick, R. J. (2008). Nucleocapsid protein function in early infection processes. *Virus Res.* **134**, 39–63.
13. Levin, J. G., Mitra, M., Mascarenhas, A. & Musier-Forsyth, K. (2010). Role of HIV-1 nucleocapsid protein in HIV-1 reverse transcription. *RNA Biol.* **7**, 754–774.
14. Ji, X., Klarmann, G. J. & Preston, B. D. (1996). Effect of human immunodeficiency virus type 1 (HIV-1) nucleocapsid protein on HIV-1 reverse transcriptase activity *in vitro*. *Biochemistry*, **35**, 132–143.
15. DeStefano, J. J. (1996). Interaction of human immunodeficiency virus nucleocapsid protein with a structure mimicking a replication intermediate. Effects on stability, reverse transcriptase binding, and strand transfer. *J. Biol. Chem.* **271**, 16350–16356.
16. Rodriguez-Rodriguez, L., Tsuchihashi, Z., Fuentes, G. M., Bambara, R. A. & Fay, P. J. (1995). Influence of human immunodeficiency virus nucleocapsid protein on synthesis and strand transfer by the reverse transcriptase *in vitro*. *J. Biol. Chem.* **270**, 15005–15011.
17. Peliska, J. A., Balasubramanian, S., Giedroc, D. P. & Benkovic, S. J. (1994). Recombinant HIV-1 nucleocapsid protein accelerates HIV-1 reverse transcriptase catalyzed DNA strand transfer reactions and modulates RNase H activity. *Biochemistry*, **33**, 13817–13823.
18. Tanchou, V., Gabus, C., Rogemond, V. & Darlix, J. L. (1995). Formation of stable and functional HIV-1 nucleoprotein complexes *in vitro*. *J. Mol. Biol.* **252**, 563–571.
19. Grohmann, D., Godet, J., Mely, Y., Darlix, J. L. & Restle, T. (2008). HIV-1 nucleocapsid traps reverse transcriptase on nucleic acid substrates. *Biochemistry*, **46**, 12230–12240.
20. Mougel, M., Houzet, L. & Darlix, J. L. (2009). When is it time for reverse transcription to start and go? *Retrovirology*, **6**, 24.
21. Post, K., Kankia, B., Gopalakrishnan, S., Yang, V., Cramer, E., Saladores, P. *et al.* (2009). Fidelity of plus-strand priming requires the nucleic acid chaperone activity of HIV-1 nucleocapsid protein. *Nucleic Acids Res.* **37**, 1755–1766.
22. Jacob, D. T. & DeStefano, J. J. (2008). A new role for HIV nucleocapsid protein in modulating the specificity of plus strand priming. *Virology*, **378**, 385–396.
23. Didierlaurent, L., Houzet, L., Morichaud, Z., Darlix, J. L. & Mougel, M. (2008). The conserved N-terminal basic residues and zinc-finger motifs of HIV-1 nucleocapsid restrict the viral cDNA synthesis during virus formation and maturation. *Nucleic Acids Res.* **36**, 4745–4753.
24. Iwatani, Y., Rosen, A. E., Guo, J., Musier-Forsyth, K. & Levin, J. G. (2003). Efficient initiation of HIV-1 reverse transcription *in vitro*. Requirement for RNA sequences downstream of the primer binding site abrogated by nucleocapsid protein-dependent primer–template interactions. *J. Biol. Chem.* **278**, 14185–14195.
25. Egele, C., Schaub, E., Ramalanjaona, N., Piemont, E., Ficheux, D., Roques, B. *et al.* (2004). HIV-1 nucleocapsid protein binds to the viral DNA initiation sequences

and chaperones their kissing interactions. *J. Mol. Biol.* **342**, 453–466.
26. Egele, C., Schaub, E., Piemont, E., de Rocquigny, H. & Mely, Y. (2005). Investigation by fluorescence correlation spectroscopy of the chaperoning interactions of HIV-1 nucleocapsid protein with the viral DNA initiation sequences. *C. R. Biol.* **328**, 1041–1051.
27. Li, X., Quan, Y., Arts, E. J., Li, Z., Preston, B. D., de Rocquigny, H. *et al.* (1996). Human immunodeficiency virus type 1 nucleocapsid protein (NCp7) directs specific initiation of minus-strand DNA synthesis primed by human tRNA(Lys3) *in vitro*: studies of viral RNA molecules mutated in regions that flank the primer binding site. *J. Virol.* **70**, 4996–5004.
28. Lener, D., Tanchou, V., Roques, B. P., Le Grice, S. F. & Darlix, J. L. (1998). Involvement of HIV-I nucleocapsid protein in the recruitment of reverse transcriptase into nucleoprotein complexes formed *in vitro*. *J. Biol. Chem.* **273**, 33781–33786.
29. Druillennec, S., Caneparo, A., de Rocquigny, H. & Roques, B. P. (1999). Evidence of interactions between the nucleocapsid protein NCp7 and the reverse transcriptase of HIV-1. *J. Biol. Chem.* **274**, 11283–11288.
30. Kati, W. M., Johnson, K. A., Jerva, L. F. & Anderson, K. S. (1992). Mechanism and fidelity of HIV reverse transcriptase. *J. Biol. Chem.* **267**, 25988–25997.
31. You, J. C. & McHenry, C. S. (1993). HIV nucleocapsid protein. Expression in *Escherichia coli*, purification, and characterization. *J. Biol. Chem.* **268**, 16519–16527.
32. Lener, D., Benarous, R. & Calogero, R. A. (1995). Use of a constrain phage displayed-peptide library for the isolation of peptides binding to HIV-1 nucleocapsid protein (NCp7). *FEBS Lett.* **361**, 85–88.
33. Divita, G., Restle, T. & Goody, R. S. (1993). Characterization of the dimerization process of HIV-1 reverse transcriptase heterodimer using intrinsic protein fluorescence. *FEBS Lett.* **324**, 153–158.
34. Thrall, S. H., Reinstein, J., Wohrl, B. M. & Goody, R. S. (1996). Evaluation of human immunodeficiency virus type 1 reverse transcriptase primer tRNA binding by fluorescence spectroscopy: specificity and comparison to primer/template binding. *Biochemistry*, **35**, 4609–4618.
35. Feng, J. Y. & Anderson, K. S. (1999). Mechanistic studies comparing the incorporation of (+) and (–) isomers of 3TCTP by HIV-1 reverse transcriptase. *Biochemistry*, **38**, 55–63.
36. Chen, Y., Balakrishnan, M., Roques, B. P., Fay, P. J. & Bambara, R. A. (2003). Mechanism of minus strand strong stop transfer in HIV-1 reverse transcription. *J. Biol. Chem.* **278**, 8006–8017.
37. Gao, L., Balakrishnan, M., Roques, B. P. & Bambara, R. A. (2007). Insights into the multiple roles of pausing in HIV-1 reverse transcriptase-promoted strand transfers. *J. Biol. Chem.* **282**, 6222–6231.
38. Vartanian, J. P., Plikat, U., Henry, M., Mahieux, R., Guillemot, L., Meyerhans, A. & Wain-Hobson, S. (1997). HIV genetic variation is directed and restricted by DNA precursor availability. *J. Mol. Biol.* **270**, 139–151.
39. Traut, T. W. (1994). Physiological concentrations of purines and pyrimidines. *Mol. Cell. Biochem.* **140**, 1–22.
40. Muriaux, D. & Darlix, J. L. (2010). Properties and functions of the nucleocapsid protein in virus assembly. *RNA Biol.* **7**, 744–753.
41. Godet, J. & Mely, Y. (2010). Biophysical studies of the nucleic acid chaperone properties of the HIV-1 nucleocapsid protein. *RNA Biol.* **7**, 687–699.
42. Cen, S., Khorchid, A., Gabor, J., Rong, L., Wainberg, M. A. & Kleiman, L. (2000). Roles of Pr55(gag) and NCp7 in tRNA(3)(Lys) genomic placement and the initiation step of reverse transcription in human immunodeficiency virus type 1. *J. Virol.* **74**, 10796–10800.
43. Hargittai, M. R., Mangla, A. T., Gorelick, R. J. & Musier-Forsyth, K. (2001). HIV-1 nucleocapsid protein zinc finger structures induce tRNA(Lys,3) structural changes but are not critical for primer/template annealing. *J. Mol. Biol.* **312**, 985–997.
44. Tisne, C., Roques, B. P. & Dardel, F. (2001). Heteronuclear NMR studies of the interaction of tRNA(Lys)3 with HIV-1 nucleocapsid protein. *J. Mol. Biol.* **306**, 443–454.
45. Cruceanu, M., Gorelick, R. J., Musier-Forsyth, K., Rouzina, I. & Williams, M. C. (2006). Rapid kinetics of protein–nucleic acid interaction is a major component of HIV-1 nucleocapsid protein's nucleic acid chaperone function. *J. Mol. Biol.* **363**, 867–877.
46. Darlix, J. L., Godet, J., Ivanyi-Nagy, R., Fosse, P., Mauffret, O. & Mely, Y. (2011). Flexible nature and specific functions of the HIV-1 nucleocapsid protein. *J. Mol. Biol.* **410**, 565–581.
47. Druillennec, S., Dong, C. Z., Escaich, S., Gresh, N., Bousseau, A., Roques, B. P. & Fournie-Zaluski, M. C. (1999). A mimic of HIV-1 nucleocapsid protein impairs reverse transcription and displays antiviral activity. *Proc. Natl Acad. Sci. USA*, **96**, 4886–4891.
48. Miller Jenkins, L. M., Hara, T., Durell, S. R., Hayashi, R., Inman, J. K., Piquemal, J. P. *et al.* (2007). Specificity of acyl transfer from 2-mercaptobenzamide thioesters to the HIV-1 nucleocapsid protein. *J. Am. Chem. Soc.* **129**, 11067–11078.
49. Morellet, N., Jullian, N., De Rocquigny, H., Maigret, B., Darlix, J. L. & Roques, B. P. (1992). Determination of the structure of the nucleocapsid protein NCp7 from the human immunodeficiency virus type 1 by 1H NMR. *EMBO J.* **11**, 3059–3065.
50. Amarasinghe, G. K., De Guzman, R. N., Turner, R. B., Chancellor, K. J., Wu, Z. R. & Summers, M. F. (2000). NMR structure of the HIV-1 nucleocapsid protein bound to stem–loop SL2 of the psi-RNA packaging signal. Implications for genome recognition. *J. Mol. Biol.* **301**, 491–511.
51. Summers, M. F., Henderson, L. E., Chance, M. R., Bess, J. W., Jr, South, T. L., Blake, P. R. *et al.* (1992). Nucleocapsid zinc fingers detected in retroviruses: EXAFS studies of intact viruses and the solution-state structure of the nucleocapsid protein from HIV-1. *Protein Sci.* **1**, 563–574.
52. Kerr, S. G. & Anderson, K. S. (1997). RNA dependent DNA replication fidelity of HIV-1 reverse transcriptase: evidence of discrimination between DNA and RNA substrates. *Biochemistry*, **36**, 14056–14063.
53. Anderson, K. S., Sikorski, J. A. & Johnson, K. A. (1988). Evaluation of 5-enolpyruvoylshikimate-3-phosphate synthase substrate and inhibitor binding by stopped-flow and equilibrium fluorescence measurements. *Biochemistry*, **27**, 1604–1610.